Photodynamic and Radiolytic Inactivation of Ion Channels Formed by Gramicidin A: Oxidation and Fragmentation†

Lars Kunz,‡ Ulrich Zeidler,‡ Klaus Haegele,§ Michael Przybylski,§ and Guenther Stark*,‡

Department of Biology and Department of Chemistry, University of Konstanz, Konstanz, Germany

Received May 8, 1995; Revised Manuscript Received July 6, 1995⊗

ABSTRACT: Ion channels formed by the peptide gramicidin A in planar lipid membranes have been reported to react very sensitively upon irradiation of the membrane by ionizing radiation (radiolysis), by UV light (photolysis), or by visible light in the presence of appropriate photosensitizers (photodynamic inactivation). In all three cases the effect is due to the presence of the four tryptophan residues of the pentadecapeptide. Modifications of these amino acids—due to an interaction with free radicals formed upon water radiolysis or due to light absorption—have been found to reduce the membrane conductance by many orders of magnitude. The present study was intended to correlate functional changes, observed at the level of single ion channels, with changes of the molecular structure identified by mass spectrometry. About 98% of the inactivated channels showed a single-channel conductance of virtually zero, while about 2% of the channels present before irradiation are converted to a state of reduced conductance (and reduced lifetime). On the structural level, irradiation in the presence of the photosensitizer Rose Bengal was found to produce oxidation and fragmentation of the peptide at the positions of the tryptophan residues. Our results provide evidence that the main effect of radiolysis, or of photodynamic treatment, is the cleavage of the peptide backbone leading to immediate closure of an open ion channel.

The action of free radicals on cellular components and its relation to certain human diseases are widely investigated at present. Our study aims at a clarification of potential molecular mechanisms by which free radicals may influence transport processes through biological membranes. To this end, their effect on certain well-known model systems is considered, the normal function of which has been analyzed in great detail in the past. We have shown in previous publications that ion channels formed by the antibiotics gramicidin A (Strässle et al., 1987, 1989; Strässle & Stark, 1992) or amphotericin B (Barth et al., 1993; Zeidler et al., 1995) respond very sensitively to the presence of free radicals generated by absorption of ionizing radiation in water (water radiolysis), or to visible light in the presence of photosensitizers (photodynamic inactivation). The present investigation is intended to provide a more detailed analysis of the functional consequences of radical action on the level of single gramicidin channels, and to correlate the functional aspects with structural changes. The linear pentadecapeptide gramicidin A is a channel-forming substance, for which detailed structural and functional information is available [see Woolley and Wallace (1992), Wallace (1992), Killian (1992), and Busath (1993) for recent reviews]. Therefore, this compound appears most appropriate for the investigation of radical-induced modifications.

Inactivation of gramicidin channels may be easily detected by conductance measurements in planar lipid membranes. The conductance induced by gramicidin A has been found to decrease by many orders of magnitude on exposure of the membrane to UV light (photolysis, Busath & Waldbillig, 1983; Jones et al., 1986; Strässle et al., 1989), to ionizing radiation (radiolysis, Stark et al., 1984; Strässle et al., 1987, 1989), or to visible light in the presence of photosensitizers (photodynamic inactivation, Strässle & Stark, 1992; Rokitskaya et al., 1993). All three effects have been shown to be due to the presence of the four tryptophan residues of gramicidin A. Photolysis may be considered as a direct radiation effect initiated by light absorption of the tryptophan chromophores. Radiolysis, on the other hand, is an indirect radiation effect caused by interaction of the radiation-induced primary $OH^{\bullet}$ and the secondary $HO_2^{\bullet}$ radicals (from water decomposition) with the tryptophan residues. Upon photodynamic inactivation, finally the excitation energy of a sensitizer—either directly or indirectly via free radicals—is eventually transferred to the tryptophan residues.

The main functional consequence of photolytic, of radiolytic, and of photodynamic tryptophan damage has been found to consist of the elimination of open ion channels. The present paper is intended to analyze further details of this process and to correlate functional and structural changes. This was achieved by functional characterization methods (inactivation kinetics, single-channel analysis, and noise analysis) combined with structural characterization of the reaction products by mass spectrometry.

EXPERIMENTAL PROCEDURES

Membrane Formation. Planar lipid membranes were formed from 0.5−1% (w/v) solutions of diphytanoyllecithin (Avanti Polar Lipids, Birmingham, AL) in *n*-decane (standard for gas chromatography; Fluka, Buchs, Switzerland) across a hole of 0.2−1 mm diameter. The latter was drilled through a diaphragm of a Lexan (polycarbonate) cuvette separating

† This work was supported by grants from the Deutsche Forschungsgemeinschaft (Az. Sta 236/4) to G.S. and (Az. Pr 175/3) to M.P.

* Address correspondence to this author at the Fakultät für Biologie, Universität Konstanz, Postfach 5560 M638, D-78434 Konstanz, Germany. FAX: +49-7531-883 183.

‡ Department of Biology.

§ Department of Chemistry.

⊗ Abstract published in *Advance ACS Abstracts,* August 15, 1995.

0006-2960/95/0434-11895$09.00/0

two aqueous solutions (pH 3) of either 1 M CsCl or 1 M NaCl (p.a. quality; Roth, Karlsruhe, Germany). Commercially available gramicidin D (Sigma Chemie, Deisenhofen, Germany), a mixture of gramicidins A, B, and C at approximate ratios of 8:1:2, was added to the membrane-forming solution. This mixture will be referred to as gramicidin A in the following (i.e., the results presented are believed to be largely identical for the three analogs). The concentration was chosen to obtain the membrane conductance desired ($10^{-7}-10^{-5}$ M for macroscopic values of the conductance, $10^{-10}-10^{-9}$ M in order to observe single-channel fluctuations). In the case of photodynamic experiments, the membrane-forming solution also contained a 0.5 mM aliquot of the dye Rose Bengal (95%, Aldrich, Steinheim, Germany). The temperature of all experiments was 21 ± 1 °C.

Irradiation Procedures. Photodynamic inactivation of gramicidin channels was studied by illuminating the membrane and its surrounding annulus with a conventional light source. The light was filtered through an IR water filter and a UV cutoff filter (Strässle & Stark, 1992). To investigate free radical-induced channel inactivation, the membrane and its aqueous environment were exposed to 80 kV X-rays. The setup has been described in previous publications (Barth & Stark, 1991; Stark 1991; Barth et al., 1993). X-ray absorption in water and the concomitant radiolysis of water molecules generate the primary radicals $OH^•$, $H^•$, and $e_{aq}^{•-}$ [see, e.g., Buxton (1987) and v. Sonntag (1987)]. In the presence of oxygen, $H^•$, and $e_{aq}^{•-}$ are converted into the secondary superoxide radical $O_2^{•-}$ and into the perhydroxyl radical $HO_2^•$. The two oxygen radicals represent a conjugated acid−base pair. The pK_a of the weak acid $HO_2^•$ is 4.8. Therefore, at pH < 4.8, the perhydroxyl radical is predominant, and at pH > 4.8, the superoxide radical is predominant. As a consequence, air-saturated solutions at sufficiently low pH essentially contain $OH^•$ and $HO_2^•$ radicals. The presence of both types of radicals is required for inactivation of gramicidin channels (Strässle et al., 1987). Radiolysis of water allows generation of well-defined concentrations, c_R, of radicals R. At a given radiation dose, D (in Gy), c_R is determined by the G_R value of the radical [$G_R(OH^•) = 2.7$; $G_R(O_2^{•-}/HO_2^•) = 3.2$] according to

$$c_R = (1.03 \times 10^{-7}\ \mathrm{M}) \times G_R \times (D/\mathrm{Gy}) \qquad (1)$$

The kinetics of inactivation were studied by following the time course of the membrane current (at a constant voltage of 50−100 mV) as a function of time after irradiation. The current, after amplification, was fed into an IBM-compatible PC equipped with analog/digital board DAS-1602 (Keithly MetraByte, Taunton, MA).

Single-Channel Experiments. Inactivation of ion channels was studied over several orders of magnitude. Starting at the macroscopic level, the membrane current was decreased until the discrete current fluctuations of single ion channels could be analyzed. A special amplifier built in our electronic workshop was used to detect the stepwise increase (or decrease) of the electric current, which is indicative of the opening (or closing) process of an ion channel. From the current fluctuations, after transfer of the digitized data into the computer, the distribution of the single-channel conductance and the mean dwell time of the open channel state were obtained. An automatic program was developed for this purpose, which was based on the software package Asyst (Keithly MetraByte).

Noise Analysis. The single-channel characteristics (i.e., conductance amplitude and mean open time of the channel) may also be obtained from a study of the electrical noise in the presence of many open ion channels (Zingsheim & Neher, 1974; Kolb et al., 1975; Kolb & Bamberg, 1977). The fluctuation of the electric current was analyzed using either the (one-sided) spectral power density, $S_I(f)$, or the autocorrelation function, $C(\tau) = \overline{[\delta J(t) \times \delta J(t+\tau)]}$. The membrane current (at constant voltage) was amplified (Model 427 of Keithly Instruments and Model 113 of Princeton Applied Research) and transferred into the computer via the analog/digital board DAS-1602. Discrete values $S_I(f_k)$ were obtained from the formula [see, e.g., Bendat and Piersol (1986)]:

$$S_I(f_k) = \frac{2\Delta t}{N n_m} \sum_{i=1}^{n_m} |\bar{I}_i(f_k)|^2 \qquad (2)$$

f = frequency, Δt = time interval of data points, N = number of data points, n_m = number of measurements, $\bar{I}_i(f_k)\Delta t$ = discrete values of the Fourier transform of the current $I(t)$, i.e.

$$\bar{I}_i(f_k) = \sum_{n=0}^{N-1} I(n\Delta t) \exp(-2\pi i k n/N), \qquad f_k = k/N\Delta t,\ k = 0, 1, ..., N-1 \qquad (3)$$

In order to avoid aliasing errors, the band width of the setup was limited according to the Nyquist frequency $f_N = 1/2\Delta t$. The following experimental settings were used throughout: Δt = 30 ms, N = 4096, n_m = 1−15. In view of the comparatively large value chosen for Δt, open channel noise (Sigworth et al., 1987) could be neglected. All calculations were performed using the software package Asyst.

Mass Spectrometry. Fast atom bombardment mass spectrometry (FAB-MS) of gramicidin A and irradiation products was obtained with a Finnigan MAT 312/AMD-500 (AMD-Intectra, Harpstedt, Germany) double-focusing magnetic sector mass spectrometer, equipped with a 24 kV cesium primary ion source. Instrumental details and conditions for acquisition of FAB spectra were as previously described (Przybylski et al., 1985; Heidman et al., 1988; Glocker et al., 1994). Gramicidin A was dissolved in methanol (300 μM). In addition, the solution contained an equimolar amount of the sensitizer Rose Bengal. Following light irradiation, *p*-nitrobenzyl alcohol as the matrix and NaI were added in equal volumes to a 40 μL sample aliquot. The resulting solution was concentrated to approximately 10 μL in a speed-vac centrifuge, put on a stainless-steel sample target, and then directly inserted into the ion source of the mass spectrometer.

^{252}Cf-plasma desorption mass spectra (PDMS) were obtained on a BioIon-20K time-of-flight spectrometer (BioIon, Uppsala, Sweden) equipped with 10 μCi of ^{252}Cf as primary ion source (Schneider et al., 1990). The sample was prepared by adding an equal volume of chloroform to the irradiated gramicidin solution (see above). An aliquot of the resulting solution was deposited on a nitrocellulose sample target.

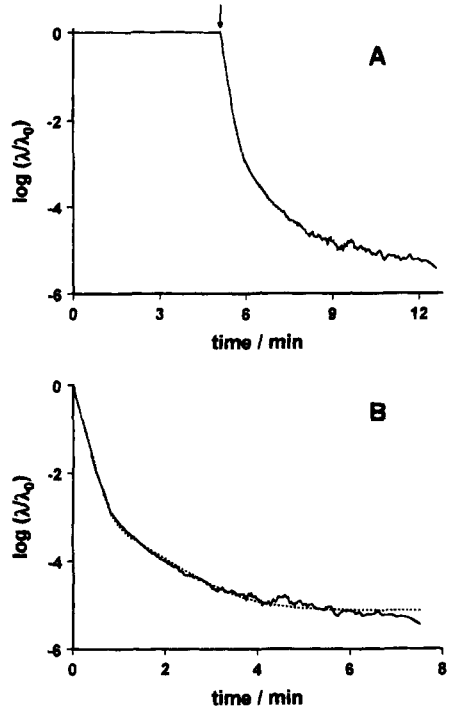

FIGURE 1: Kinetics of the decay of the conductance, λ, after the start of illumination (arrow) with visible light of a membrane in the presence of the dye Bengal Rose (the time-independent conductance, λ_0, in the absence of illumination was 7.3×10^{-5} S). (A) Original data. (B) Analysis of the conductance decay. Zero time corresponds to the onset of illumination. The dashed line is a fit of eq 4 to the data with the following values of the parameters: $\tau_1 = 6.65$ s, $\tau_2 = 38.24$ s, $a = 0.00239$, $c = 7.54 \times 10^{-6}$.

RESULTS

Functional Consequences of Irradiation. The conductance of pure lipid membranes separating aqueous solutions of NaCl, or CsCl, is known to be extremely small (i.e., of the order of 10^{-8}–10^{-6} S cm^{-2}). This is a consequence of the very low solubility of inorganic ions in the hydrophobic membrane interior. The addition of small amounts of the peptide gramicidin A, either to the aqueous phases or to the membrane-forming solution, gives rise to a drastic increase by many orders of magnitude of the membrane conductance. This is the result of the formation of porelike ion channels by the peptide which allow the free passage of alkali ions, as was first shown by Hladky and Haydon (1972). The discrete fluctuations of the membrane current observed by these authors at extremely low peptide concentrations have been interpreted as the opening and closing of ion channels. The strongly enhanced membrane conductance induced by gramicidin A in lipid membranes may be eliminated by irradiation of the membrane and its aqueous environment by X-rays, by UV light, or by visible light in the presence of the dye Rose Bengal as a photosensitizer. The decrease is due to the elimination of open ion channels formed by gramicidin A. This may be concluded from the appearance of the characteristic conductance fluctuations—indicative of the presence of only a few open channels—after the membrane has been irradiated for a sufficiently long period of time. The effect is illustrated by photodynamic inactivation of the membrane conductance (Figure 1). The mean value, $\bar{\Lambda}$, of the conductance increment induced by single gramicidin channels is 36.5 pS under the experimental conditions applied (see below). Therefore, the time-

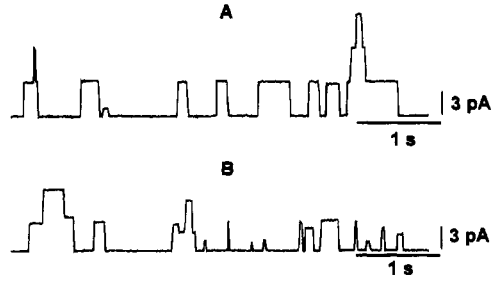

FIGURE 2: Current tracings representing the opening and closing of ion channels formed from gramicidin A in diphytanoyllecithin membranes at a constant applied voltage of 100 mV (1 M CsCl in water, pH 3, band width 100 Hz, sample rate 200 s^{-1}). (A) Control. (B) A membrane (with a conductance equivalent to about 900 open channels) was irradiated by X-rays until the typical current fluctuations of single ion channels became apparent.

independent initial conductance, λ_0, of 7.3×10^{-5} S corresponds to 2×10^6 open gramicidin channels. There is a decrease by more than 5 orders of magnitude after about 10 min of illumination. Increase of the electrical noise at this time is due to the statistical fluctuations of 10–20 channels between their open and closed states. After further illumination, the conductance is reduced to show the typical fluctuations of single ion channels (cf. Figure 2).

The decay of the conductance, λ, may be formally described by the equation:

$$\lambda(t)/\lambda_0 = [(1 - a)\exp(-t/\tau_1) + a\exp(-t/\tau_2) + c]/(1 + c) \quad (4)$$

The first 2 orders of magnitude of the decay may be fitted by a single-exponential term with the characteristic time constant, τ_1 (Figure 1B). There is, however, clear evidence for the presence of a second exponential term of comparatively small amplitude. The constant, c, accounts for the final conductance, $\lambda_f = \lambda_0 c/(1 + c)$, of the membrane after complete inactivation of the ion channels ($c \ll 1$).

Equation 4 is in line with a simple model of inactivation (see below), which is based on two parallel reaction pathways:

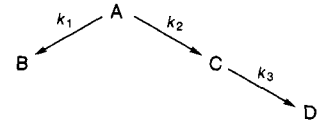

The model assumes that photodynamic inactivation converts part of the active ion channels (state A) into an inactive state, B, of zero conductance. The rest of the channels are transformed into state C. This is a state of lower, but nonzero, channel conductance, which may become completely inactivated (state D) by a second light-dependent step. The model is certainly a simplification of a more complicated phenomenon (see below). It is, however, in line with the shape of the inactivation kinetics (Figure 1), with the results of the single-channel studies (Figures 2–5), and with the analysis of the electrical noise (Figures 6–7).

The existence of an intermediate channel state, C, may be directly deduced from the single-channel fluctuations shown in Figure 2. The fluctuations induced by the residual channels after irradiation by X-rays (Figure 2B) show a number of events of smaller current amplitude. Though such events are also present at the control, they represent very

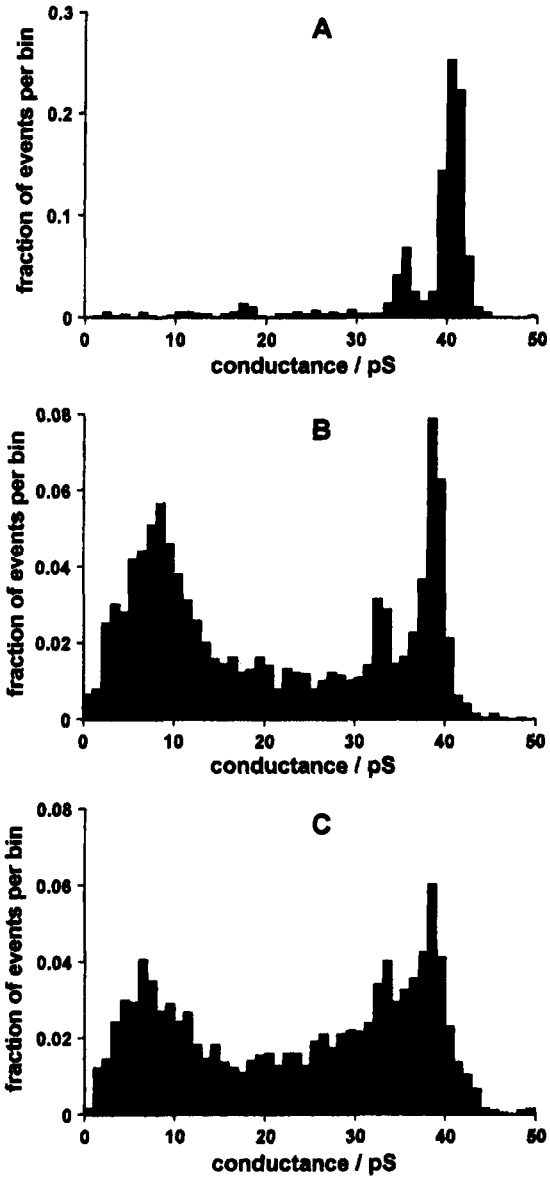

FIGURE 3: Distribution of the amplitudes of single-channel fluctuations of gramicidin A ion channels before and after photodynamic or radiolytic inactivation. The relative number of events per bin (i.e., per a conductance interval of 1 pS = 10^{-12} A/V) is plotted as a function of the channel conductance, Λ. (A) Control (cf. Figure 2A): Analysis of 607 discrete conductance fluctuations in the absence of irradiation (mean value, $\bar{\Lambda}$ = 37.3 pS). (B) Photodynamic inactivation: A membrane containing about 10^5 open channels was irradiated until the single-channel behavior (2805 events similar to Figure 2B) could be analyzed. The mean value, $\bar{\Lambda}$, of the fluctations was 20.8 pS in this case. (C) Radiolytic inactivation: The conductance of a membrane (originally containing about 2400 open channels) was reduced to the single-channel level (2154 events similar to Figure 2B, mean value, $\bar{\Lambda}$ = 23.6 pS).

rare processes, whose frequency is clearly increased by irradiation. The same behavior was observed after photodynamic inactivation. There is an enhanced probability for the observation of smaller current amplitudes, which is evident when the distributions of the fluctuation amplitudes of the current are compared (Figure 3). Normal (unmodified) gramicidin A shows a pronounced peak at about 40−42 pS and a smaller peak around 35−36 pS (from contaminations with gramicidins B and C). There is a broad background of events with smaller amplitude. The occurrence rate of these "mini-channels" is, however, comparatively small [see Busath and Szabo (1981) and Sawyer et al. (1990) for a discussion of this problem]. The amplitude histogram of photodynamically inactivated, or radiolyzed gramicidin A, on the other hand, contains a comparatively broad maximum culminating around 8−10 pS, in addition to the normal maxima. The new maximum is assigned to state C of the reaction scheme (see above). On further irradiation of the membrane, the single-channel fluctuations were found to disappear. This is interpreted as a transition of the intermediate state, C, into an inactive state, D. It cannot be excluded that this transition occurs via one or several additional conducting channel states, as has been suggested in the case of photolytic inactivation (Busath & Waldbillig, 1983). The comparatively broad distribution of low conductance amplitudes would be consistent with such an assumption. The finding of a relatively broad maximum might, however, also indicate that the intermediate species, C, consists of different chemical species reflecting several parallel pathways of inactivation. For the sake of simplicity, the possible heterogeneity of C is neglected in the forthcoming analysis.

The proposed channel state, C, shows a reduced dwell time. Figure 4 indicates that the fraction of open channels of normal gramicidin A (after transition into the open state) decays exponentially with time. This is indicative of a largely uniform mean dwell time (of about 600 ms) of the open channel state. The corresponding decay of the number of open channels after radiolytic or photodynamic inactivation requires a sum of two exponential terms (at least) for an adequate description. Therefore, these channels represent two classes (at least) with different mean dwell times. The data in Figure 4 were obtained by analysis of current traces similar to Figure 2B (i.e., by analysis of channels in state C and of residual channels in state A). The time constant τ_2 (within a factor of 2) agrees with that of unirradiated channels. The time constant τ_1 is smaller by a factor of 4−6. τ_1 is caused by channels in state C, as was found by separate analysis of low-conductance single-channel events.

The combination of the single-channel data and of the kinetic experiments allows to determine the rate constants of the model. The decay of the conductance after photodynamic inactivation of gramicidin channels (Figure 1) may be calculated by application of standard kinetic techniques. The reaction scheme predicts the same time dependence of the conductance (cf. eq 4) as has been observed experimentally (apart from the final radiation insensitive conductance of the pure lipid membrane not included in the model, i.e., $c = 0$). The constants τ_1, τ_2, and a are obtained as

$$\tau_1 = \frac{1}{k_1 + k_2}, \tau_2 = \frac{1}{k_3}, a = \frac{\Lambda_C}{\Lambda_A} \frac{k_2}{k_1 + k_2 - k_3} \qquad (5)$$

Λ_A and Λ_C represent the mean conductance values of the open channel in states A and C, respectively. Equation 5 was derived with the condition that the aggregation behavior of gramicidin A (e.g., the dimerization reaction) is not relevant to the photodynamic inactivation. This means that the channels in states A and C are assumed to fluctuate between their respective closed and open conformations (for a justification, see Discussion).

Equation 5 allows determination of the rate constants k_1, k_2, and k_3 as a function of the experimental quantities τ_1, τ_2,

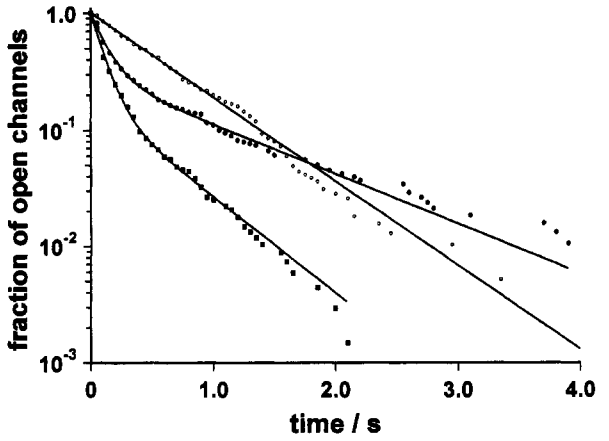

FIGURE 4: Dwell time of open gramicidin A ion channels before and after photodynamic or radiolytic inactivation (normalized survivor plot). Zero time corresponds to the opening of the channels. The solid lines represent a fit of the data to the equation: $\alpha_1 \exp(-t/\tau_1) + \alpha_2 \exp(-t/\tau_2)$. (○) Control: 385 single events, $\alpha_1 = 1$, $\tau_1 = 602$ ms, $\alpha_2 = 0$. (●) 377 single events after photodynamic inactivation of 14 000 open channels: $\alpha_1 = 0.7$, $\tau_1 = 130$ ms, $\alpha_2 = 0.3$, $\tau_2 = 1014$ ms. (■) 677 single events after radiolytic inactivation of 8700 open channels: $\alpha_1 = 0.82$, $\tau_1 = 106$ ms, $\alpha_2 = 0.18$, $\tau_2 = 525$ ms.

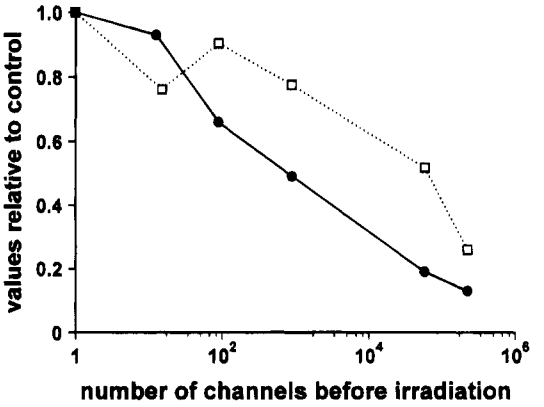

FIGURE 5: Mean values of the channel conductance (□) and of the channel dwell time (●) after radiolysis of a different number of channels as measured by the single-channel method (for experimental conditions, see Figure 2). Control values: $\bar{\Lambda} = 36.5 \pm 0.5$ pS, $\tau = 610 \pm 33$ ms.

a, Λ_A, and Λ_C. The mean values obtained from 22 independent measurements are $k_1 = 0.16\ s^{-1}$, $k_2 = 4.0 \times 10^{-3}\ s^{-1}$, $k_3 = 0.034\ s^{-1}$. The data hold for the light intensity employed. The ratio, $P_C = k_2/(k_1 + k_2)$, is, however, independent of the intensity and allows estimation of the relative importance of the two reaction paths. P_C corresponds to the probability of formation of the intermediate state C during photodynamic inactivation. The comparatively small value of $P_C = 2.4 \times 10^{-2}$ indicates that inactivation via state C represents a side reaction. About 98% of the inactivation events proceed by direct transition of the fully active state A into the inactive state B.

The analysis was confirmed by two independent qualitative approaches. The main conclusion, namely, the comparatively rare occurrence of channels in state C, was tested by the single-channel analysis and by analysis of the electrical noise of a multipore system: If a small number (of the order of 10) of channels in the normal state A is inactivated to observe the fluctuations of an individual channel, the probability for this channel to be in the intermediate state C is small (less than 22%). For that reason, the single-channel histogram obtained from such an experiment will mainly show fluctuations of large amplitude, which are characteristic of residual intact channels; i.e., the histogram will resemble the control shown in Figure 3A. The probability of observing channels in state C during this procedure (i.e., the relative height of the maximum at 10 pS) is expected to increase with the number of original channels before irradiation. This was qualitatively confirmed throughout our single-channel studies, and is illustrated by Figure 5. Both the mean values of the channel conductance, $\bar{\Lambda}$, and of the channel dwell time, τ, were found to decrease with increasing number of channels before irradiation. This is consistent with the smaller values of the single-channel conductance, and of the channel dwell time in state C. Though qualitatively correct, the data do not, however, allow a quantitative analysis: In view of the comparatively long period of time required for the measurement of a sufficient number of single-channel fluctuations, the diffusion of intact gramicidin molecules from the torus of the membrane cannot be neglected. As a consequence, there is a significant overestimation of the number of channels in state A throughout this kind of measurements (cf. Figure 3B,C). It was found, however, that the effect of diffusion is small enough to be neglected in the measurement of inactivation kinetics (Figure 1).

Single-channel properties may also be obtained from a multipore system by analysis of the spectral power density, $S_I(f)$, or of the autocorrelation function, $C(\tau)$, of the electric current. Following Kolb and Bamberg (1977), the spectral power density, $S_I(f)$, of the current noise induced by the opening and closing of intact gramicidin channels is of a Lorentzian-type:

$$S_I(f) = \frac{S_I(0)}{1 + (f/f_c)^2},\ S_I(0) = 4\sigma^2\tau_c, f_c = 1/2\pi\tau_c \qquad (6)$$

$\sigma^2 = \overline{(\delta I)^2}$, variance. The correlation time, τ_c, is related to the corner frequency, f_c, and (according to the fluctuation dissipation theorem) corresponds to the relaxation time of the system. The single-channel conductance, Λ, is obtained from the relation:

$$\Lambda = \frac{\sigma^2}{\bar{I}V} \qquad (7)$$

$\bar{I}$ = mean current at the applied voltage V. Equation 7 is an approximation, the validity of which is restricted only at very high membrane conductances, λ. A further important prerequisite of this equation is the presence of a population of channels having uniform values of their single-channel conductance. Equation 7 may, however, be applied in a qualitative way in order to indicate a shift of the mean channel conductance to lower values, if a new population of reduced conductance appears throughout channel inactivation (e.g., channels belonging to the intermediate state C). The relevant experiments are illustrated in Figures 6 and 7. Figure 6 shows a typical power spectrum of intact gramicidin channels. It compares well with the previous results of Kolb and Bamberg (1977). The shape of $S_I(f)$ was found to remain largely identical during the inactivation process. The value of $S_I(0) = 4\tau_c\bar{\Lambda}\bar{I}V$ (cf. eqs 6 and 7), however, is reduced by many orders of magnitude. Figure 7 illustrates the behavior

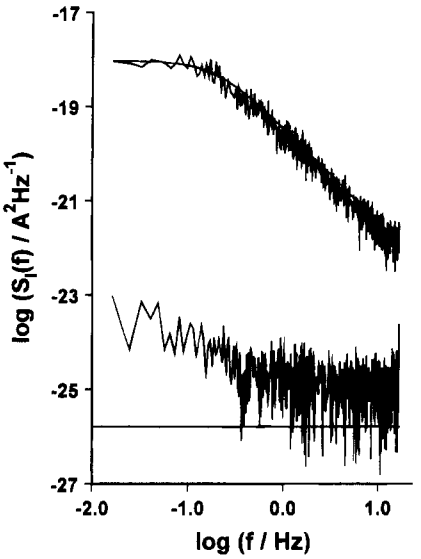

FIGURE 6: Spectral power density of the current noise as a function of frequency at a constant voltage of 100 mV. Upper trace: Analysis of the current across a diphytanoyllecithin membrane of 0.3 mm diameter separating aqueous solutions of 1 M CsCl and an appropriate amount of gramicidin A to ensure a mean membrane conductance of 7×10^{-7} S. The data represent averages of five successive spectra requiring a total time of 10.24 min ($n_m = 5$, cf. eq 2). The theoretical curve represents a fit of eq 6 to the data with the following parameters: $S(0) = 9.4 \times 10^{-19}$ A^2 Hz^{-1}, $f_c = 0.19$ Hz. Lower trace: This control experiment shows the response of a lipid membrane in the absence of gramicidin A (membrane conductance $< 7 \times 10^{-11}$ S) with a resistor of 10^6 Ω in parallel (average of two spectra). The solid line represents the level of the thermal noise for this resistor calculated according to the Nyquist relation.

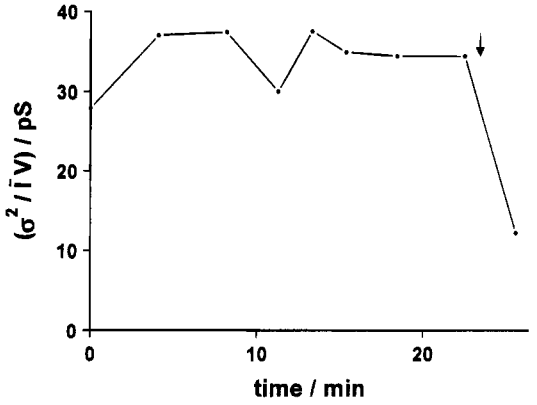

FIGURE 7: Change of the quantity $\sigma^2/(\bar{I}V)$ (cf. eq 7) after photodynamic inactivation of gramicidin channels (see text for details). At the arrow, the specific membrane conductance (7×10^{-4} S cm^{-2}), through illumination in the presence of Rose Bengal, was reduced by 2 orders of magnitude.

of $\sigma^2/\bar{I}V$ as a function of time. Applying eq 7, this quantity should remain constant irrespective of the value of $\bar{I}$, if the mean channel conductance, $\bar{\Lambda}$, does not change throughout the inactivation process. There is, however, a steep decrease of this quantity after photodynamic reduction of the conductance by 2 orders of magnitude. This may be considered a confirmation of the generation of channel species with lower conductance values during irradiation.

Therefore, all three functional methods applied are compatible with the assumption of an intermediate species C. The probability of formation of this species is, however, rather small. The predominant radiation effect is the direct

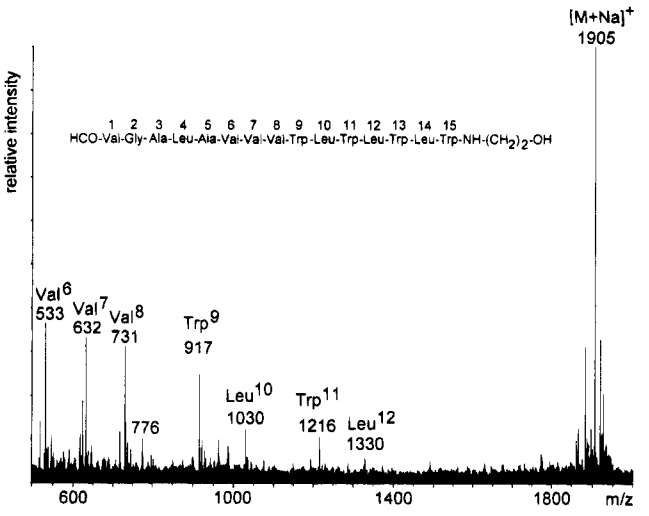

FIGURE 8: Fast atom bombardment (FAB) mass spectra of intact gramicidin A.

transition of the channels from the fully active state A into the inactive state B.

Most of the data presented refer to photodynamic inactivation. Similar results were also obtained from the radiolysis of gramicidin channels. In the case of photolysis, states of low channel conductance were first described by Busath and Waldbillig (1983).

Mass Spectrometric Identification of Oxidation and Degradation Products. The effect of the photodynamic treatment on the structure of gramicidin A was studied by fast atom bombardment (FAB) mass spectrometry. This technique has been employed previously as a powerful method for the precise molecular weight and complete primary structure determination of peptaibols and related polypeptide antibiotics (Rinehart et al., 1982; Brückner et al., 1983; Przybylski et al., 1984). Figure 8 shows the FAB mass spectrum (positive ions) of intact (untreated) gramicidin A from a methanol solution, obtained with *p*-nitrobenzyl alcohol (NBOH) as the matrix solvent, to which sodium iodide had been added. The most abundant ion is the sodiated molecular ion $[M + Na]^+$ observed at *m/z* 1905 (M_r 1882; $[M+H]^+$ at *m/z* 1883 otherwise, without NaI addition). The accompanying ions may be attributed to contaminating analogs of gramicidin A. Furthermore, a series of sequence-specific, N-terminal fragment ions are found, which formally arise by cleavage of $C_\alpha - C_{CO}$ bonds (or of peptide bonds and subsequent CO elimination) and appear as Na adducts. These ions enable the exact determination of a large part of the sequence from the N-terminus and have been used previously to elucidate the structure of peptaibols (Przybylski et al., 1984, 1985). In the case of Figure 8, ions at *m/z* 533, 632, 731, 917, 1030, 1216, and 1330 represent the partial sequences Val^6 to Leu^{12}. Relative to these sequence-specific FAB-induced fragmentations, other ions formed by hydrolysis at peptide bonds [such as the N-terminal fragment HCO-(1−8) by cleavage at the Val^8/Trp^9 bond] are found only with low intensities.

FAB spectra obtained from gramicidin A samples after photodynamic treatment for 10, 55, and 75 min are compared in Figure 9A−C. Significant changes and degradation were already clearly observed after 10 min of irradiation as indicated by the drastic decrease in intensity of the molecular ion peak at *m/z* 1905. Instead of the pattern observed in

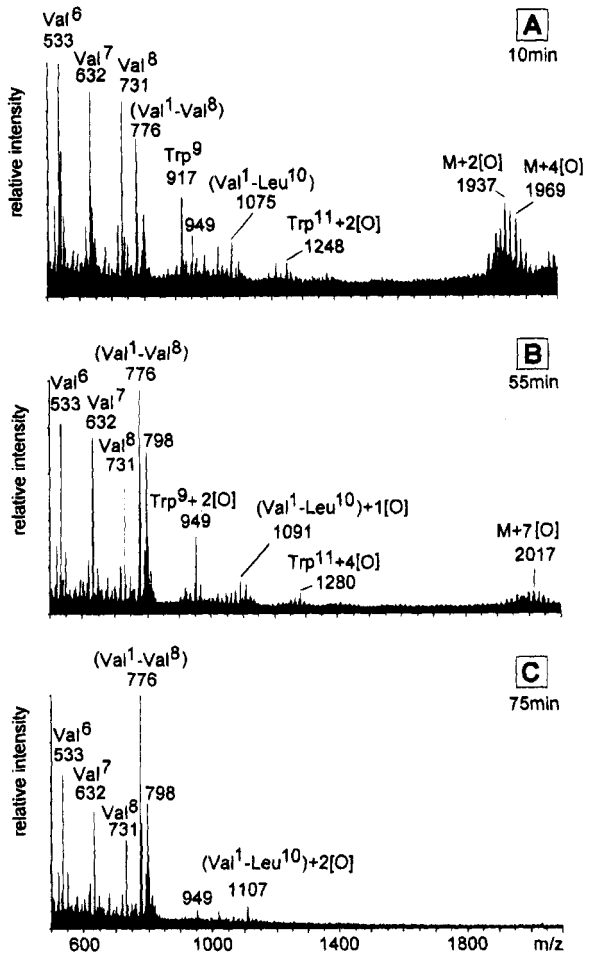

FIGURE 9: Fast atom bombardment (FAB) mass spectra of gramicidin A after different times of irradiation by visible light in the presence of Rose Bengal: (A) 10 min, (B) 55 min, (C) 75 min. Some important ions are labeled as follows: FAB-induced fragments are designated by the C-terminal amino acid (e.g., Val^6, see also Figure 8). Photodynamically induced fragments are denoted by the first and the last member of the sequence (e.g., Val^1-Val^8).

Figure 8, a series of molecular ions representing oxidation products appear with masses separated by multiples of 16 amu, respectively, showing incorporation of up to at least six oxygen atoms (e.g., *m/z* 1921, 1937, 1953, 1969, and 1985 in Figure 9A). Moreover, the mass shifts and changes of the fragmentation pattern provide evidence for the oxidations occurring at Trp residues. Thus, N-terminal fragments up to Val^8 (m/z *731*) were found unchanged, while the fragment ion resulting from cleavage at Trp^9 is shifted to *m/z* 949, equivalent to the formal addition of O_2 (as are other subsequent fragments comprising Trp^{11} and Trp^{13} residues).

Extension of the irradiation times (Figure 9B,C) resulted in further oxidation, as shown by the appearance of higher oxidized molecular ions. The peak at *m/z* 1216 is shifted to *m/z* 1280, equivalent to the formal addition of two O_2 molecules to the fragment HCO-Val^1-Trp^{11} (i.e., one O_2 molecule per Trp residue). The most important result of an extended irradiation time is, however, the complete disappearance of the molecular ion $[M+Na]^+$, which is indicative of photodynamic fragmentation of the peptide. Furthermore, the direct identification of the fragmentation pathway is provided by the increasing abundance, with increasing time, of ions at *m/z* 776 and 798, resulting from specific peptide cleavage between Val^8 and Trp^9. Like all molecular ions of the intact peptide, these ions represent the sodium salt and its $[M+Na]^+$ form, due to the presence of NaI in the matrix. Other N-terminal ions are unchanged. There is additional strong evidence that the photodynamic degradation specifically involves the Trp residues of the peptide: All peptide fragments identified only comprise the partial sequence (1–8), and the C-terminal fragments (containing the four Trp residues of gramicidin A) are detectable neither in the mass region *m/z* 250–500 (data not shown) nor above *m/z* 500 (cf. Figure 9).

The characteristic photodynamic modifications of gramicidin A by initial oxidation of the intact peptide, and subsequent fragmentation, were corroborated by ^{252}Cf-plasma desorption mass spectra (data not shown).

DISCUSSION

Gramicidin A is a linear pentadecapeptide with tryptophan residues at positions 9, 11, 13, and 15: HCO-L-Val-Gly-L-Ala-D-Leu-L-Ala-D-Val-L-Val-D-Val-L-Trp-D-Leu-L-Trp-D-Leu-L-Trp-D-Leu-L-Trp-NHC_2H_4OH. The helical dimer formed by association of two monomers is generally believed to represent an important principle of the formation of hydrophilic, ion-permeable channels through the bimolecular lipid phase of biological membranes. The four Trp residues have been found to be involved in channel inactivation by UV light, by X-rays, or by visible light in the presence of a suitable sensitizer. In the case of photolysis, the involvement of the Trp residues was deduced from a correlation of the decay of the Trp fluorescence and of the conductance induced by gramicidin A (Jones et al., 1986). The efficiency of radiolytic or photosensitized inactivation was found to decrease by several orders of magnitude, if the Trp residues were replaced by other aromatic residues such as phenylalanine or naphthylalanine (Strässle et al., 1987, 1989; Strässle & Stark, 1992). Therefore, photolysis, radiolysis, and photodynamic inactivation of gramicidin channels may be assumed to originate from a chemical modification of the tryptophans.

There are numerous reports on the radiolysis of the amino acid tryptophan (Jayson et al., 1954; Peter & Rajewsky, 1963; Armstrong & Swallow, 1969) and on tryptophan-containing peptides and proteins (Aldrich & Cundall, 1969; Winchester & Lynn, 1970; Masuda et al., 1971; Schuessler & Herget, 1984; Simpson et al., 1992). A great variety of different reaction products has been found. Side chain modifications and fragmentation through cleavage of the peptide bond are major changes observed at the molecular level of peptides and proteins. Degradation of the side chains also represents the most important chemical change during the photosensitized oxidation of biomolecules (Straight & Spikes, 1985). The cleavage of peptide bonds, however, seems to occur only rarely in photooxidation, and has been reported only for lumiflavin-sensitized photooxidation of lysozyme (Gomyo & Fujimaki, 1970). Gramicidin A seems to represent another exception in this respect (see below).

Inactivation of gramicidin channels by X-rays was found to be initiated by free radicals of water radiolysis (Strässle et al., 1987, 1989). The conclusion was based on the analysis of the shape of inactivation curves and on the kinetics of inactivation in the absence and in the presence of radical scavengers. The data were consistent with the assumption

that channel inactivation is initiated by subsequential attack of a $OH^{\bullet}$ radical (or of a secondary radical produced by $OH^{\bullet}$) and of a $HO_2^{\bullet}$ radical at a single tryptophan residue of gramicidin A. The nature of the reaction path finally leading to channel inactivation has so far, however, remained obscure. The same holds for photolytic or photodynamic inactivation, where the events after light absorption by the tryptophans or by the sensitizer are largely unclear. In the case of the latter both, type I and type II processes have been suggested depending on the nature of the sensitizer (Strässle & Stark, 1992; Rokitskaya et al., 1993).

The results of the present study yield some definite molecular information on the final state of inactivated channels. The observation of fragmentation, after irradiation of gramicidin A with visible light in the presence of the sensitizer Rose Bengal, provides a simple explanation for the transition of gramicidin channels from the normal state A into the inactivated state B. The cleavage of a peptide bond may be expected to interrupt the diffusion path of the cations through the channel, therefore explaining the direct transition to values of the single-channel conductance of virtually zero (as was observed for the predominant part of the inactivation events).

This conclusion is independent from the detailed structure of the open channel, which is generally assumed to consist of a helical dimer formed by head-to-head association of two monomers. The kinetics of association of gramicidin monomers have been neglected so far. The data presented may be interpreted without making definite assumptions about the equilibrium between the channel structure and its monomeric elements (i.e., the equilibrium constant may or may not depend on the extent of fragmentation generated). The shape of the inactivation curves could be described by a simple reaction scheme neglecting the association equilibrium of gramicidin monomers (cf. Figure 1B). The same result has been obtained previously in the case of radiolytic inactivation of gramicidin A (Strässle et al., 1989). There is further support for the assumption that the association equilibrium is of secondary relevance for the inactivation process: Busath and Hayon (1988) applied photolytic light flashes in order to study the kinetics of inactivation. The main part of the current decrease occurred within less than 100 μs, i.e., within a time scale much shorter than the kinetics of channel formation and dissociation.

The first structural modification, induced by irradiation and observed by mass spectrometry, is the oxidation of the peptide taking place at the tryptophan residues. This is concluded from the absence of oxidations at those fragments which do not contain tryptophans. Furthermore, the maximum number of O_2 molecules added to the fragments seems to correspond to their number of tryptophan residues. The functional consequence of these oxidations is uncertain at present (see below). We suspect, however, that oxidation precedes fragmentation at the corresponding amino acid residue of the peptide.

While state B of the reaction scheme may be explained by fragmentation of the channel, the structural differences between channel states A and C remain unclear. In view of its heterogeneity (see last section), state C might consist of a series of different reaction products which arise from side chain modifications of the tryptophan residues. In any case, the occurrence of state C is a rare event; i.e., the direct transition into state B is by far the most important process. This holds at least for the radiolytic and photodynamic inactivation the present analysis is based on.

The correlation (as described above) between the functional channel states A, B, and C and the structures found by mass spectrometry needs further discussion. One might argue that the main transition A → B (observed upon channel inactivation) is the consequence of a chemical transformation of the tryptophan residues preceding fragmentation of the peptide; i.e., fragmentation is not required for inactivation. This argument is supported by the finding that the "channel forming activity" of gramicidin A is strongly reduced if the tryptophan residues are replaced by other aromatic amino acid residues. Therefore, a comparatively small modification of the tryptophan side chains might be sufficient for complete inactivation of the channels. The importance of the tryptophans has been explained by two alternative hypotheses. Both of them have in common that the presence of the tryptophan residues favors the structural alignment of gramicidin dimers (in order to form open ion channels). Stark et al. (1986) suggested that the conductive pathways through the gramicidin dimers are only opening if the dimers are stabilized by formation of lateral aggregates (which are thought to be favored by tryptophan−tryptophan contacts between adjacent dimers). Becker et al. (1991), on the other hand, emphasized that hydrogen bond formation between the tryptophans of isolated dimers and the polar membrane−water interface is responsible for the stabilization. Irrespective of the kind of dimer stabilization, chemical modification of the tryptophans may be expected to reduce the formation rate of open ion channels, and would, therefore, decrease the conductance induced by gramicidin A. The question, whether the fragmentation of the peptide is a necessary condition for the transition A → B, or whether a chemical transformation (preceding fragmentation)—such as oxidation or formation of short-lived intermediates not detected by mass spectrometry—is sufficient, cannot be answered definitely by the existing data. In any case, the observation of fragmentation allows a simple and straightforward interpretation of irreversible channel inactivation.

Radiolysis—in view of the more complicated procedure required—has not been investigated by mass spectrometry so far. Irradiation must be performed in the presence of water in this case (e.g., by using gramicidin A containing lipid vesicles). Subsequently, gramicidin A and its irradiation products would have to be separated from the surrounding lipid phase and would have to be transferred to an organic solvent. In view of the largely identical functional behavior of photodynamically and X-ray-inactivated gramicidin channels, we expect the same main structural consequence in both cases, namely, fragmentation of the peptide backbone.

In summary, the essential molecular event at the photosensitized inactivation of gramicidin channels is shown to be the fragmentation of the peptide at the site of the tryptophan residues. In view of the largely identical functional inactivation behavior, this is also inferred for inactivation induced by ionizing radiation. It remains to be established whether this result may be generalized to other tryptophan-containing ion channels, or whether fragmentation is a consequence of a special property of gramicidins A, B, and C, namely, of the close spatial proximity of four (or at least three) tryptophan residues.

ACKNOWLEDGMENT

We thank Mrs. Martina Jetschke for the measurement of some supplementary ^{252}Cf-plasma desorption mass spectra of gramicidin A.

REFERENCES

Aldrich, J. E., & Cundall, R. B. (1979) *Int. J. Radiat. Biol. 16*, 343−358.
Armstrong, R. C., & Swallow (1969) *Radiat. Res. 40*, 563−579.
Barth, C., & Stark, G. (1991) *Biochim. Biophys. Acta 1066*, 54−58.
Barth, C., Stark, G., & Wilhelm, M. (1993) *Biophys. J. 64*, 92−97.
Becker, M. D., Greathouse, D. V., Koeppe, R. E., II, & Andersen, O. S. (1991) *Biochemistry 30*, 8830−8839.
Bendat, J. S., & Piersol, A. G. (1986) *Random Data, Analysis and Measurement Procedures*, p 392, Wiley & Sons, New York.
Brückner, H., Jung, G., & Przybylski, M. (1983) *Chromatographia 17*, 679−685.
Busath, D. D. (1993) *Annu. Rev. Physiol. 55*, 473−501.
Busath, D., & Szabo, G. (1981) *Nature 294*, 371−373.
Busath, D. D., & Waldbillig, R. C. (1983) *Biochim. Biophys. Acta 736*, 28−38.
Busath, D. D., & Hayon, E. (1988) *Biochim. Biophys. Acta 944*, 73−78.
Buxton, G. V. (1987) in *Radiation Chemistry* (Farhataziz & Rodger, M. A. J., Eds.) pp 321−349, VCH Publishers, New York.
Glocker, M., Borchers, C., Fiedler, W., Suckau, D., & Przybylski, M. (1994) *Bioconjugate Chem. 5*, 583−590.
Gomyo, T., & Fujimaki, M. (1970) *Agric. Biol. Chem. 34*, 302−309.
Heidmann, M., Fonrobert, P., Przybylski, M., Platt, K. H., Seidel, A., & Oesch, F. (1988) *Biomed. Mass Spectrom. 15*, 329−334.
Hladky, S. B., & Haydon, D. A. (1972) *Biochim. Biophys. Acta 274*, 294−312.
Jayson, G. G., Scholes, G., & Weiss, J. (1954) *Biochem. J. 57*, 386−390.
Jones, D., Hayon, E., & Busath, D. D. (1986) *Biochim. Biophys. Acta 861*, 62−66.
Killian, J. A. (1992) *Biochim. Biophys. Acta 1113*, 391−425.
Kolb, H.-A., & Bamberg, E. (1977) *Biochim. Biophys. Acta 464*, 127−141.
Kolb, H.-A., Läuger, P., & Bamberg, E. (1975) *J. Membr. Biol. 20*, 133−154.
Masuda, T., Ovadia, J., & Grossweiner, L. I. (1971) *Int. J. Radiat. Biol 20*, 447−459.
Peter, G., & Rajewsky, B. (1963) *Z.f.Naturforsch. 18B*, 110−114.
Przybylski, M., Dietrich, I., Manz, I., & Brückner, H. (1984) *Biomed. Mass Spectrom. 11*, 569−582.
Przybylski, M., Manz, I., Fonrobert, P., Dietrich, I., & Brückner, H. (1985) *Adv. Mass Spectrom. 10*, 1519−1521.
Rinehart, K. L., Gandiosi, L. A., Moore, M. L., Pandey, R. C., Cook, J. C., Barber, M., Sedgwick, R. D., Bordoli, R. S., Tyler, A. N., & Green, B. N. (1982) *J. Am. Chem. Soc. 103*, 6517-6520.
Rokitskaya, T. I., Antonenko, Y. N., & Kotova, E. A. (1993) *FEBS Lett. 329*, 332−335.
Sawyer, D. B., Koeppe, R. E., II, & Andersen, O. S. (1989) *Biochemistry 28*, 6571−6583.
Schneider, K., Nielsen, P. F., Suckau, D., & Przybylski, M. (1990) in *Mass Spectrometry of Large Non-Volatile Molecules* (Hilf, E., Ed.) pp 176−193, World Scientific, London.
Schuessler, H., & Herget, A. (1984) *Int. J. Radiat. Biol 37*, 71−80.
Sigworth, F. J., Urry, D. W., & Prasad, K. U. (1987) *Biophys. J. 52*, 1055−1064.
Simpson, J. A., Narita, S., Gieseg, S., Gebicki, S., Gebicki, J. M., & Dean, R. T. (1992) *Biochem. J. 282*, 621−624.
Stark, G. (1991) *Biochim. Biophys. Acta 1071*, 103−122.
Stark, G., Strässle, M., & Wilhelm, M. (1984) *Biochim. Biophys. Acta 775*, 265−268.
Stark, G., Strässle, M., & Takácz (1986) *J. Membrane Biol. 89*, 23−37.
Strässle, M., & Stark, G. (1992) *Photochem. Photobiol. 55*, 461−463.
Strässle, M., Stark, G., & Wilhelm, M. (1987) *Int. J. Radiat. Biol. 51*, 265−286.
Strässle, M., Stark, G., Wilhelm, M., Daumas, P., Heitz, F., & Lazaro, R. (1989) *Biochim. Biophys. Acta 980*, 305−314.
Straight, R. C., & Spikes, J. D. (1985) in *Singlet Oxygen* (Frimer, A. A., Ed.) Vol. IV, pp 91−143, CRC Press, Boca Raton, FL.
v. Sonntag, C. (1987) *The Chemical Basis of Radiation Biology*, Taylor & Francis, London.
Wallace, B. A. (1992) *Prog. Biophys. Mol. Biol. 57*, 59−69.
Winchester, R. V., & Lynn, K. R. (1970) *Int. J. Radiat. Biol. 17*, 541−548.
Woolley, G. A., & Wallace (1992) *J. Membr. Biol. 129*, 109−136.
Zeidler, U., Barth, C., & Stark, G. (1995) *Int. J. Radiat. Biol. 67*, 127−134.
Zingsheim, H. P., & Neher, E. (1974) *Biophys. Chem. 2*, 197−207.

BI951029W